Spinterface effects in hybrid La_0.7Sr_0.3MnO_3 /SrTiO_3 /C_60 /Co magnetic tunnel junctions

Ilaria Bergenti, Takeshi Kamiya, Dongzhe Li, Alberto Riminucci, Patrizio Graziosi, Donald A Maclaren, Rajib K Rakshit, Manju Singh, Mattia Benini, Hirokazu Tada, et al.

Spinterface effects in hybrid $La_{0.7}Sr_{0.3}MnO_3$ /$SrTiO_3$ /C_{60}/Co magnetic tunnel junctions

Journal:	*ACS Applied Electronic Materials*
Manuscript ID	el-2022-00300p.R3
Manuscript Type:	Article
Date Submitted by the Author:	10-Aug-2022
Complete List of Authors:	Bergenti, Ilaria; CNR, ISMN Kamiya, Takeshi; Osaka university, Engineering Science Li, Dongzhe; CEMES, Physics Riminucci, Alberto; ISMN CNR Graziosi, Patrizio; CNR, ISMN MacLaren, Donald; SUPA Rakshit, Rajib; CSIR, National Physical Laboratory Singh, Manju; CSIR, National Physical Laboratory Benini, Mattia; CNR, ISMN Tada, Hirokazu; Osaka University Graduate School of Engineering Science School of Engineering Science , Division of Materials Physics Smogunov, Alexander; CNRS - SPEC/SPCSI, CEA Saclay IRAMIS Dediu, Valentin; Institute of Nanostructured Materials Support Unit of Bologna

Spinterface effects in hybrid $La_{0.7}Sr_{0.3}MnO_3$ /$SrTiO_3$ /C_{60}/Co magnetic tunnel junctions

Ilaria Bergenti[1], Takeshi Kamiya[2], Dongzhe Li[3] Alberto Riminucci[1], Patrizio Graziosi[1], Donald .A. MacLaren[4], Rajib K. Rakshit [5], Manju Singh [5], Mattia Benini[1], Hirokazu Tada[2], Alexander Smogunov[6], Valentin A. Dediu[1]*

[1] Institute of Nanostructured Materials ISMN-CNR, Via Gobetti 101, Bologna 40129, Italy

[2] Department of Materials Engineering Science, Osaka University, 1-3, Machikaneyama, Toyonaka, Osaka, Japan, 560-8531

[3] CEMES, Université de Toulouse, CNRS, 29 rue Jeanne Marvig, F-31055 Toulouse, France

[4] SUPA, School of Physics and Astronomy, University of Glasgow, Glasgow G12 8QQ

[5] CSIR - National Physical Laboratory, Dr. K. S. Krishnan Marg, New Delhi, 110012, India

[6]Service de Physique de l'Etat Condensé (SPEC), CEA, CNRS, Université Paris-Saclay, CEA Saclay 91191 Gif-sur-Yvette Cedex, France

e-mail: ilaria.bergenti@cnr.it

Abstract:

The orbital hybridization at the Co/C_{60} interface has proved to strongly enhance the magnetic anisotropy of the cobalt layer, promoting such hybrid systems as appealing components for sensing and memory devices. Correspondingly, the same hybridization induces substantial variations in the ability of Co/C_{60} interface to support spin polarized currents and can bring out spin filtering effect. The knowledge of the effects at both sides shall allow for a better and more complete understanding of interfacial physics. In this paper we investigate the Co/C_{60} bilayer in the role of spin polarized electrode in the $La_{0.7}Sr_{0.3}MnO_3$/$SrTiO_3$/C_{60}/Co configuration, thus substituting the bare Co electrode in the well-known $La_{0.7}Sr_{0.3}MnO_3$/$SrTiO_3$/Co magnetic tunnel junction. The study revealed that the spin polarization (SP) of the tunneling currents escaping from the Co/C_{60} electrode is generally negative, i.e. inverted with respect to the expected SP of the Co electrode. The observed sign of the spin polarization was confirmed via DFT calculations by considering the hybridization between cobalt and molecular orbitals.

Keywords: *tunnel junction, spinterface, molecular spintronics, C60, hybrid interface, spin-dependent density of states*

INTRODUCTION

The formation of a hybridized layer at the interface between ferromagnetic metals and organic semiconductors has resulted efficient for the modulation of the magnetic and spin properties of both components[1,2]. An illustrative example is represented by the interface between the pure carbon allotrope buckminsterfullerene (C_{60}) and ferromagnetic 3d metals[3–5], like Co. Orbital hybridization at the interface between a C_{60} overlayer and an epitaxial ultra thin film of Co(0001) leads to a considerable change in the magnetic anisotropy of the Co[6], able to induce a magnetization reorientation transition from in-plane to out-of-plane in the ferromagnetic layer and a magnetic hardening[7]. Correspondingly, the non-magnetic C_{60} molecule is also modified[8] becoming spin active by acquiring a net magnetic moment as a consequence of coupling of the carbon atoms closest to the underlying Co.

These unusual features liven up the Co/C_{60} interface as fascinating element for the modulation of the spin functionality in solid-state devices: the magnetic hardening of a FM layer, obtained by interfacing it by the organic molecule, is of technological interest in spintronic memories[9] as well as the induced spin selectivity at the interface is fundamental for the spin injection [10]. In this regards, spin transport has been proved to depend on the coupling of C_{60} molecules on magnetic surface in case of fcc-Co(111)/C_{60} [11] and Cr(001)/C_{60} [12].

Here we prove that Co/C_{60} interface can be integrated in prototypical Magnetic Tunnel Junction (MTJ) $La_{0.7}Sr_{0.3}MnO_3$/ $SrTiO_3$/Co (LSMO/STO/Co) [13] resulting in a change of the spin tunneling current of the device. We address this issue by inserting an ultra thin C_{60} molecular layer at the interface with the ferromagnetic Co layer acting as spin polarized electrode and by comparing the magnetotransport properties of LSMO/STO/C_{60}/Co MTJ with those of the reference LSMO/STO/Co MTJ. Given that spin polarized tunneling in MTJ depends on the band structure of the insulating barrier, on the properties of ferromagnetic layers and even more critically on those of their interfaces, the investigation of TMR values and sign together with the calculation of spin conductance in MTJ provides thus a direct method to test the spin polarization at the C_{60}/Co interface allowing to unlock potential applications of Co/C_{60} interface in solid state spintronic devices.

EXPERIMENTAL METHODS

A. Experiment

Cross-bar LSMO/STO/Co and LSMO/STO/C_{60}/Co were obtained by shadow masking technique on single crystal $NdGaO_3$ (NGO) (110) substrates. 15nm thick LSMO layer were deposited by channel spark ablation method following the procedure described by Graziosi et al.[14]. The STO tunneling barrier (5 nm) was grown with the same CSA technique in O_2 atmosphere (10^{-2} mbar) keeping the substrate at 700 °C. The Co top contact was obtained by e-gun evaporation in UHV ($P<10^{-9}$mbar) at

Room Temperature. The 2nm thick C_{60} layer was deposited on STO by thermal evaporation with a ultra-low flux MBKomponente cell with the growth rate of 0.15 Å/s. The Co top contact was obtained by e-gun evaporation in UHV ($P<10^{-9}$mbar) at room temperature. C_{60} was not damaged by the fabrication of the top Co electrode[15]. Metallic contacts were provided by gold pads evaporated on the LSMO and the Co electrodes. Junctions were 500 μm × 500 μm in size. The overall structures are depicted in Figures 1a and 1b

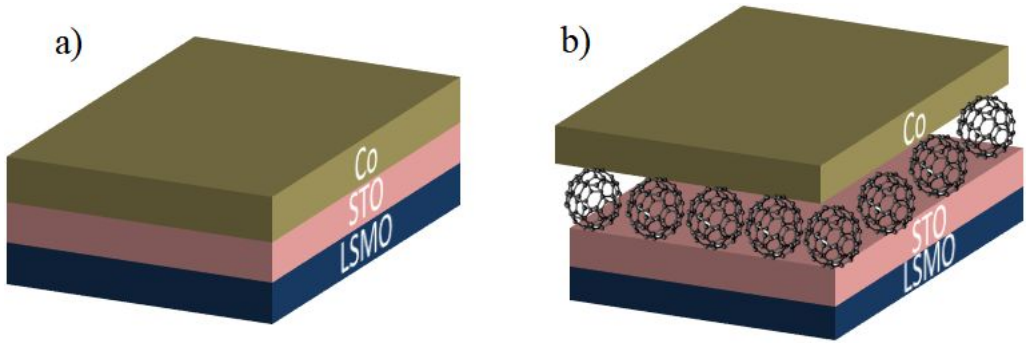

Figure.1 Schematic drawing of MTJ junctions. a) Reference device $La_{0.7}Sr_{0.3}MnO_3/SrTiO_3/Co$ b) C_{60} seeded MTJ

Transmission electron microscopy (TEM) was employed for structural characterization, using a probe-corrected JEOL ARM200cF instrument that was operated at 200 kV and was equipped with a cold field emission electron gun and a Gatan Quantum electron energy loss spectrometer. Cross-sectional samples were prepared using standard 'lift-out' procedures on an FEI Nova Nanolab Focused Ion Beam instrument.

The topography of C_{60} films was investigated by using an AFM Smena microscope (NT-MDT, Moscow, Russia) in non contact mode (NCM) under ambient conditions. Silicon cantilevers were employed.

The spin transport measurements were performed using an exchange gas cryostat, equipped with an electromagnet. A van der Pauw configuration was adopted to minimize the contributions from the electrode resistances. The TMR was measured by sweeping the magnetic field in the plane of the device, while applying a various constant biases through the junction by using a Keithley 2400 SMU in the temperature range 100 K-300 K, with a maximum applied field of μ_0H=0.9 T. The LSMO electrode was biased while the Co was grounded.

B. Density functional theory calculations

We performed spin-polarized *ab initio* calculations using the plane wave electronic structure package Quantum ESPRESSO [16] in the framework of the density functional theory (DFT). We used Perdew-Burke-Ernzerhof parametrization (PBE) for exchange-correlation functionals and we used the

ultrasoft pseudopotential formalism. Energy cut-offs of 30 Ry and 300 Ry were employed for the wavefunctions and the charge density, respectively. The C_{60}/ferromagnetic interface was simulated using a seven-layer slab of hcp-Co (0001) and a 4×4 in-plane periodicity. The full system was first relaxed fixing four Co bottom layers at their bulk positions and using 2×2 **k**-points mesh, then the electronic properties of the relaxed structure have been studied using a finer 6×6 mesh of **k**-points. The same computational parameters as in ref. [17] were used.

RESULTS AND DISCUSSION

The high-resolution transmission electron microscopy (HR-TEM) cross-section image of LSMO(15nm)/STO(5nm)/Co(50nm) confirms the excellent morphology of MTJ. Figure2a clearly shows that LSMO is epitaxial with (100) orientation over the NGO (110) substrate, as well as over the epitaxial STO layer. The Co was polycrystalline as expected for room temperature deposition. Images revealed an abrupt epitaxial LSMO/STO interface and a less sharp STO/Co one as shown by the EELS scan performed along the cross-section of the sample (Figure 2b).

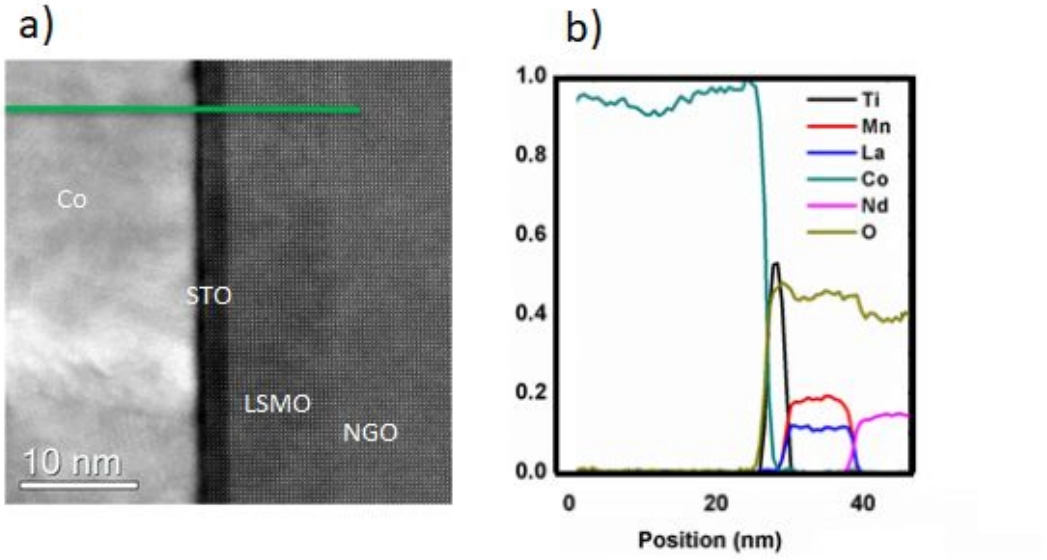

Figure 2 a) TEM cross section image of LSMO/STO/Co junction. The STO layer is completely crystalline, along with the LSMO and NGO. b) EELS analysis of the LSMO/STO/Co junction along the green line.

The insertion of C_{60} layer is obtained by depositing the organic layer onto the LSMO/STO. The STO tunnel barrier surface exhibit a smooth surface (RMS < 0.3nm, i.e. STO lattice parameter- **see SI1**). After the growth of 2nm C_{60}, the molecules form clusters distributed on the STO surface with an overall roughness of about 1 molecular layer (RMS =0.7±0.1 nm) as shown in Figure 3. At closer

inspection, AFM height profiles (see SI1) indicate a quite uniform coverage of the surface with an estimated coverage of 98%.

Subsequently, the Co deposition is performed. The partial intermixed layer between Co and C_{60} is unavoidable given the RMS of C_{60} layer, but several works pointed out that the quite compact nature of C_{60} molecule prevents the diffusion of the Co ion into the molecule[1518] Moreover during the Co growth, C60 molecule maintains its integrity[19] and molecular cluster tend to be incapsulated beneath the Co film. It is worth noting that even in case of sub-monolayer deposition[20], C_{60} layer has been used as buffer layer in Organic Light Emitting Diodes to improve efficiently the qualities of interface with metals by changing the interfacial work functions and the energy level alignment [21]

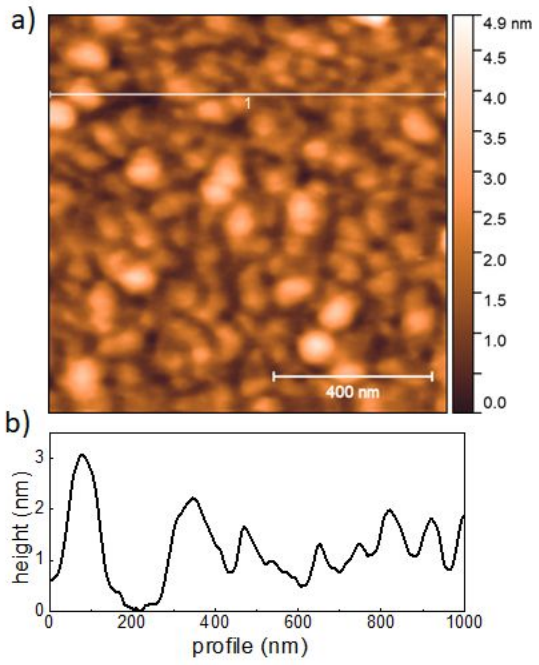

Figure 3. a)Topography of 2nm C_{60} film grown on STO substrate at room temperature b) Line profile measurement along the white line shown in (a)

Once addressed the role of C_{60} as decoupling layer between Co and STO, we now address transport data measured in the current-perpendicular-to-plane (CPP) geometry. Conduction across the LSMO/STO/Co heterostructure exhibits typical features expected for a tunneling conduction process (see SI2) ruling out any possible ohmic path. The magnetoresitance response at 100K measured under a bias of V=−0.1V corresponds to a typical MTJ butterfly curve (Fig.4a). The magnetic switching of both LSMO and Co layers is observed, showing coercive fields of around ±85 Oe for LSMO and ±200 Oe for Co. This difference allows for an antiparallel magnetic alignment between the two magnetic electrodes for intermediate magnetic fields. In agreement with previous studies[22–24], a lower-resistance state is measured in the antiparallel magnetic configuration when sweeping the field,

displaying a negative TMR value of 6%, where the TMR is defined as is defined as TMR= $\frac{R_{AP}-R_P}{R_P}$ where R_{AP} is the resistance in the antiparallel alignment of magnetizations of the electrodes and R_P is the resistance in the parallel one. According to the Julliere's model TMR is governed by the electron spin polarizations of two magnetic electrodes (P_1 and P_2) so that TMR= $\frac{2P_1P_2}{1-P_1P_2}$. This simplified picture does not consider the complexity of electronic band structure of ferromagnet and the nature of tunnel barrier and the formation of spin dependent interfacial states[25] that turns out to be of fundamental importance in the description of tunneling phenomena included the LSMO/STO/Co MTJ[13]. Considering that the densities of states for Co and LSMO are both positive[22], the inverse TMR at negative bias has been interpreted in terms of interfacial hybridization between Co atoms and STO barrier producing a change in the Co tunneling spin polarization. The hybridization at the Co/STO interface due to the formation of covalent bonding of Co and O atoms induces a magnetic moment on the interfacial Ti atoms which is aligned antiparallel to the magnetic moment of the Co layer[26]. This leads to a negative spin polarization of tunneling across the STO barrier from the Co electrode, inverting the spin polarization at the LSMO/STO interface and hence the TMR signal.

The insertion of a 2 nm thick C_{60} layer acting as a decoupling layer between Co and STO does not change the MR sign, having the hybrid LSMO/STO/C_{60}/Co MTJ still a negative TMR (Fig4b). While the magnetic switching of LSMO is located to similar field values observed for the reference LSMO/STO/Co MTJ, i.e. ±90 Oe , the switching of Co layer is broader, as a results of the increased Co roughness due to the presence of C_{60} layer underneath. We emphasized the role of the interfaces between the tunneling layer and the FM metals in favoring a particular spin polarization and electronic character of the tunneling current: STO/C_{60}/Co interface results in a negative polarization in analogy to STO/Co interface. Since the negative sign of the TMR in LSMO/STO/Co MTJs comes from the inversion of the spin polarization at the STO/Co interface, we conclude that the C_{60}/Co interface also features the inversion of the spin polarization and that the electronic structure at the Co surface is modified by the interaction with the C_{60} molecule. This result is in agreement with Moorsoom et al, [8] who observed a charge transfer at the Co/C_{60} interface associated with an induced moment in C_{60} molecules antiferromagnetically aligned to the moment of the bulk cobalt and resulting in a behavior analogous to Ti atoms at the STO/Co interface. The inversion of polarization at the Co/C_{60} interface was demonstrated also in AlO_x based MTJ[11] and in Co/C_{60}/Co purely molecular junction[27], in agreement with our findings. We also observed that in case of C60 layer, TMR value is higher than the TMR reported for MTJs with STO only, reaching nearly 11%.

The TMR effect in both cases decreases with increasing temperature and disappears at nearly RT (SI3), in agreement with most studies performed on other MTJ with LSMO and Co electrodes[28],

which could be a result of either the decrease of the spin polarization of LSMO at the interface with STO[29] and/or the spin-independent tunneling through impurity levels in the barrier activated upon increasing the temperature [30]

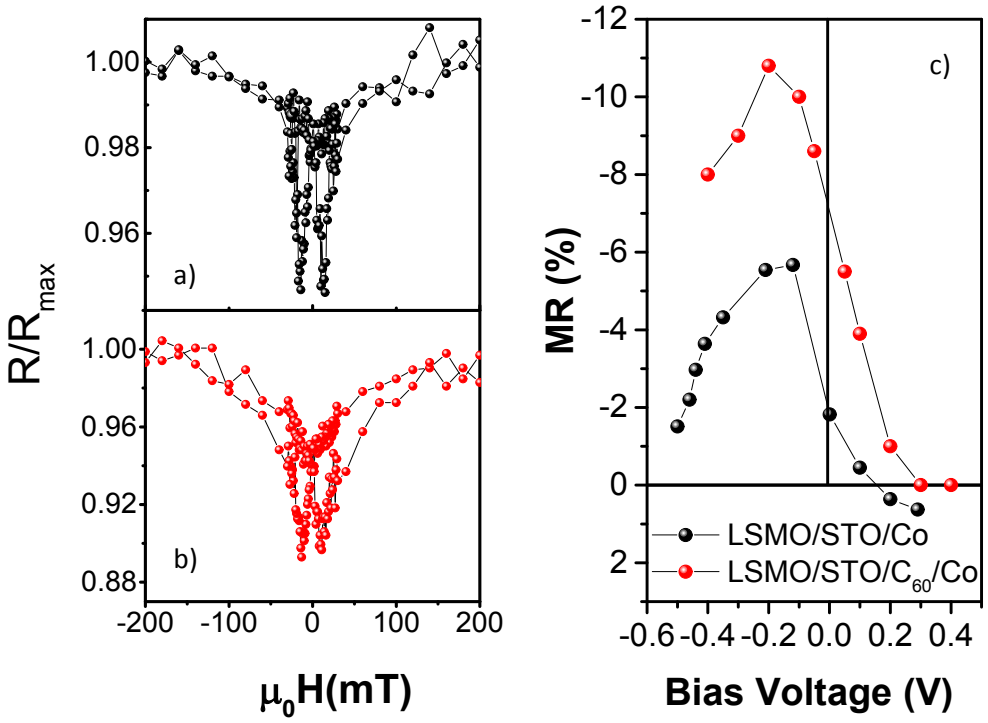

Figure 4. Negative Tunneling magnetoresistance (TMR) as a function of applied field for the two junctions LSMO/STO/Co(a) and LSMO/STO/C_{60}/Co(b) measured with voltage bias of 100 mV (c) TMR ratio as a function of the applied dc bias for LSMO/STO/Co junctions (black balls) and LSMO/STO/C_{60}/Co (red balls). Errors bars are within the symbol size.

In addition to the sign, interfaces were found to be critical for the definition of the bias dependence of TMR. In the reference LSMO/STO/Co MTJ, the maximum magnetoresistance value is at negative bias voltage (V_b=-0.1V) and the TMR features a cross over from negative to positive magnetoresistance at above the V_b =+0.2 V threshold value as we observed in Fig 4c (black balls). This TMR trend is in a good agreement with previous works with some minor differences, possibly related to sample quality variations [31]. This peculiar bias dependence of the reference MTJ has been ascribed to the structure of the DOS of the d band of Co as described by De Teresa et al.[22] and to the contribution of non resonant tunneling events trough specific defect states induced by the O vacancies in the barrier[24].

The insertion of C_{60} layer results in a different voltage dependence of the TMR, showing only larger negative magnetoresistance in the whole measured bias interval, as shown in Figure 4c(red balls). The bias dependence remains asymmetric with a maximum absolute value at V_b= -0.2V and vanishing

TMR for high positive biases. A clue for the interpretation of the bias dependent behavior of LSMO/STO/C_{60}/Co MTJ can be found in our previous *ab initio* calculations on the C_{60} adsorbed on Co [17]. As pointed out previously, a magnetic moment, antiferromagnetically aligned to the Co layer, is induced on the C_{60} molecule and correspondingly a decrease of the spin moment of the surface Co atoms beneath the molecule is expected due to hybridization with molecular states. It is worth noting that such calculations refer to C_{60} deposited on single crystal Co surface while in our devices the geometry is reversed due to the deposition of polycrystalline Co on the molecular C_{60} layer. This may induce bias asymmetry effects, similar to those detected in Co/Al_2O_3/Co[31], where non symmetric bias dependence was ascribed to the different crystalline structures of two electrodes.

To better clarify the role of Co/C_{60} in MTJ, we now implement those calculations by evaluating the tunneling probability across the interface. Calculations are carried out using the most stable configuration corresponding to C_{60} adsorbed on epitaxial Co layer in the pentagon-hexagon edge 5:6 bonding as was found in [12]. Figure 5a presents the spin-resolved DOS projected on C_{60} molecule (see for more details [17]), it is clearly spin polarized at the E_F which would potentially lead to high TMR values due to spin-split hybridized states (coming mostly from C_{60} lowest unoccupied molecular orbital, LUMO) at the metal-ferromagnetic interface. This finding is in agreement with the experimental observation of a higher TMR signal for C_{60} based MTJ. In order to better understand the transport properties of the C_{60}/Co interface and to make a better connection to the experiment, we compute the spin-resolved conductance (Figure 5b), defined as the corresponding projected DOS (PDOS) integrated over the energy interval [E_F, eU] divided by the bias voltage U, $G = \int_{EF}^{EF+eU} PDOS(E)dE/U$. This simplified approach allowed to make tractable our complex problem of spin-polarized transport across full LSMO/STO/C_{60}/Co junction, assuming that all spin-dependence comes from the Co/C_{60} interface. Two main assumptions were therefore made: i) the DOS of LSMO was supposed to be constant in energy (and so could be taken out of the energy integral); ii) similarly, the tunneling rate of all electronic states across the STO barrier is assumed to be the same and energy-independent. These assumptions, expected to work fine at small bias, can be less justified further from the Fermi energy (where, for example, additional minority spin DOS of LSMO appears, [32]) which may explain a worse agreement between experimental and theoretical results for increasing bias. Considering the LSMO/STO as a perfect spin up injector[13,22], the TMR of the full junction should depend on the ratio of spin up/down conductances, as represented in Figure 5c. Calculated this way, the TMR curve reproduces experimental data satisfactorily: calculated TMR is essentially negative and slightly asymmetric with respect to the bias voltage and rapidly decreasing with an increasing bias voltage (it is predicted also to become positive at voltages higher than the ones measured experimentally, U>4 V). Nevertheless, this simulation does not reproduce the position of

TMR maximum, which has been experimentally found at V=-0.2V while calculations place it at positive bias. These discrepancies can be ascribed to the approximations done in our calculations. Indeed, the employed LSMO/STO and Co/C_{60} band structures were based on ideal interfaces without defects and disorder, preventing a precise quantitative comparison with the experimental data collected in polycrystalline samples. Also, considering the absence of TMR inversion and the TMR intensity, the decoupling of STO and Co by the insertion of C_{60} should limit the role of O vacancies in STO in tunneling process. This could prevent the scattering and the loss of parallel angular momentum conservation [23] observed also in defective amorphous STO barrier[33] and plausibly responsible for the increase of TMR signal in our devices.

Note that the interfacial hybridization between Co and C_{60} is limited to the first molecular layer, and the derived effects and properties do not depend on the thickness of the organic layer when the devices operate in the tunneling regime.

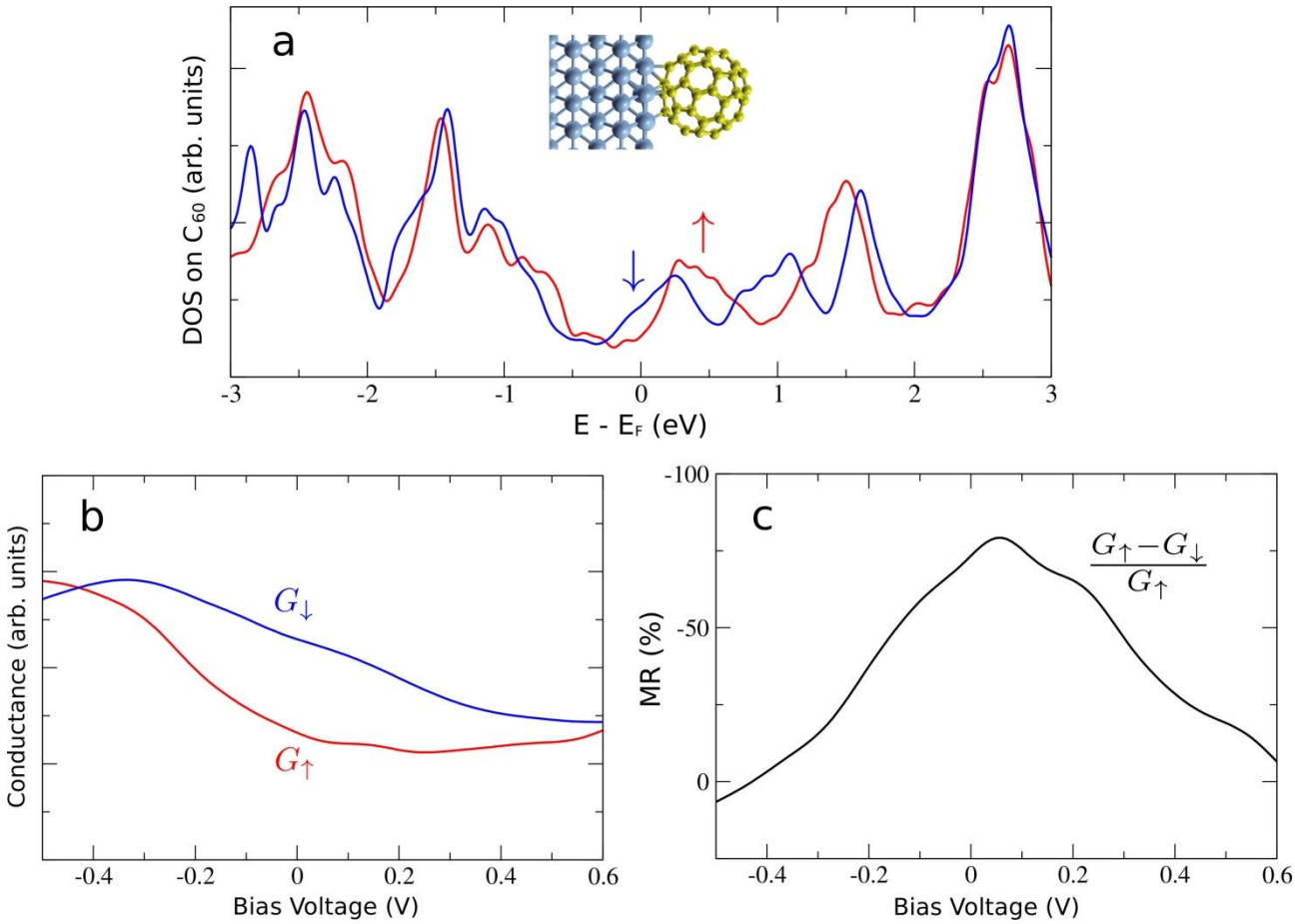

Figure.5 hcp-Co/C_{60} interface with C_{60}in (5:6)-bond adsorption geometry: a) Spin-resolved PDOS on the C_{60} molecule; b) Spin-resolved conductance calculated from the integrated PDOS; c) Calculated interface TMR $(G_{\uparrow}\text{-}G_{\downarrow})/G_{\uparrow}$. Spin-up and -down components in a) and b) are plotted in blue and red, respectively. In b) and c) negative/positive voltage corresponds to probing occupied/unoccupied states.

CONCLUSIONS

In this work, we have shown that the insertion of an ultrathin layer of C_{60} between Co and STO in MTJs strongly affects the TMR response. The substitution in LSMO/STO/Co/ tunnel junctions of the Co spin injecting electrode by Co/C_{60} induces a negative sign of TMR for the whole interval of measured voltage biases, eliminating the well-known effect of the sign change in the prototypical inorganic device, the latter confirmed also in this study on a reference sample. The DFT calculations, performed for ideal case of C_{60} adsorbed on epitaxial Co layer, clearly revealed that the negative sign of TMR is induced by the spin-dependent electronic hybridization at the Co/C_{60} interface, rather pronounced in the lowest energy adsorption geometry (with C_{60} adsorbed by the pentagon-hexagon 5:6 edge). Notably, the differences between the shapes of calculated and measured voltage dependences of SP are expected to be at least partly caused by the polycrystalline and defective nature of the investigated interfaces, but the presence of more complex and still unknown interfacial effects cannot be ruled out.

Our results demonstrate that hybrid ferromagnetic/molecular interfaces offer versatile routes for tuning of the TMR strength and sign in MTJs, enhancing the choice of spintronic device solutions for logic and memory applications.

Supporting Information. AFM characterization of C_{60} molecules adsorbed on STO, Temperature-dependent I–V characteristics of LSMO/STO/Co MTJ, Temperature dependence of the Magnetoresistance.

Aknowledgement: This paper is supported by European Union's Horizon 2020 Research and Innovation programme under grant agreement No 965046, FET-Open project Interfast (Gated INTERfaces for FAST information processes) and No 964396 FET-Open SINFONIA (Selectively activated INFOrmation technology by hybrid Organic Interfaces). RKR and MS acknowledge the receipt of fellowship from the ICTP Programme for Training and Research in Italian Laboratories, Trieste, Italy. DL acknowledges the HPC resources from CALMIP (Grant 2021-P21008).

References

(1) Bergenti, I.; Dediu, V. Spinterface: A New Platform for Spintronics. *Nano Materials Science* **2019**, *1* (3), 149–155. https://doi.org/10.1016/j.nanoms.2019.05.002.

(2) Cinchetti, M.; Dediu, V. A.; Hueso, L. E. Activating the Molecular Spinterface. *Nature Mater* **2017**, *16* (5), 507–515. https://doi.org/10.1038/nmat4902.

(3) Sharangi, P.; Pandey, E.; Mohanty, S.; Nayak, S.; Bedanta, S. Spinterface-Induced Modification in Magnetic Properties in Co40Fe40B20/Fullerene Bilayers. *J. Phys. Chem. C* **2021**, *125* (45), 25350–25355. https://doi.org/10.1021/acs.jpcc.1c08656.

(4) Han, X.; Mi, W.; Wang, X. Spin Polarization and Magnetic Properties at the C60/Fe4N(001) Spinterface. *J. Mater. Chem. C* **2019**, *7* (27), 8325–8334. https://doi.org/10.1039/C9TC02342A.

(5) Mallik, S.; Mohd, A. S.; Koutsioubas, A.; Mattauch, S.; Satpati, B.; Brückel, T.; Bedanta, S. Tuning Spinterface Properties in Iron/Fullerene Thin Films. *Nanotechnology* **2019**, *30* (43), 435705. https://doi.org/10.1088/1361-6528/ab3554.

(6) Bairagi, K.; Bellec, A.; Repain, V.; Chacon, C.; Girard, Y.; Garreau, Y.; Lagoute, J.; Rousset, S.; Breitwieser, R.; Hu, Y.-C.; Chao, Y. C.; Pai, W. W.; Li, D.; Smogunov, A.; Barreteau, C. Tuning the Magnetic Anisotropy at a Molecule-Metal Interface. *Phys. Rev. Lett.* **2015**, *114* (24), 247203. https://doi.org/10.1103/PhysRevLett.114.247203.

(7) Bairagi, K.; Bellec, A.; Repain, V.; Fourmental, C.; Chacon, C.; Girard, Y.; Lagoute, J.; Rousset, S.; Le Laurent, L.; Smogunov, A.; Barreteau, C. Experimental and Theoretical Investigations of Magnetic Anisotropy and Magnetic Hardening at Molecule/Ferromagnet Interfaces. *Phys. Rev. B* **2018**, *98* (8), 085432. https://doi.org/10.1103/PhysRevB.98.085432.

(8) Moorsom, T.; Wheeler, M.; Mohd Khan, T.; Al Ma'Mari, F.; Kinane, C.; Langridge, S.; Ciudad, D.; Bedoya-Pinto, A.; Hueso, L.; Teobaldi, G.; Lazarov, V. K.; Gilks, D.; Burnell, G.; Hickey, B. J.; Cespedes, O. Spin-Polarized Electron Transfer in C60 Interfaces. *Phys. Rev. B* **2014**, *90* (12), 125311. https://doi.org/10.1103/PhysRevB.90.125311.

(9) Hirohata, A.; Yamada, K.; Nakatani, Y.; Prejbeanu, I.-L.; Diény, B.; Pirro, P.; Hillebrands, B. Review on Spintronics: Principles and Device Applications. *Journal of Magnetism and Magnetic Materials* **2020**, *509*, 166711. https://doi.org/10.1016/j.jmmm.2020.166711.

(10) Liang, S.; Geng, R.; Yang, B.; Zhao, W.; Chandra Subedi, R.; Li, X.; Han, X.; Nguyen, T. D. Curvature-Enhanced Spin-Orbit Coupling and Spinterface Effect in Fullerene-Based Spin Valves. *Sci Rep* **2016**, *6* (1), 19461. https://doi.org/10.1038/srep19461.

(11) Wang, K.; Strambini, E.; Sanderink, J. G. M.; Bolhuis, T.; van der Wiel, W. G.; de Jong, M. P. Effect of Orbital Hybridization on Spin-Polarized Tunneling across Co/C60 Interfaces. *ACS Appl. Mater. Interfaces* **2016**, *8* (42), 28349–28356. https://doi.org/10.1021/acsami.6b08313.

(12) Shao, Y.; Pang, R.; Pan, H.; Shi, X. Fullerene/Layered Antiferromagnetic Reconstructed Spinterface: Subsurface Layer Dominates Molecular Orbitals' Spin-Split and Large Induced Magnetic Moment. *J. Chem. Phys.* **2018**, *148* (11), 114704. https://doi.org/10.1063/1.5012926.

(13) De Teresa, J. M.; Barthélémy, A.; Fert, A.; Contour, J. P.; Montaigne, F.; Seneor, P. Role of Metal-Oxide Interface in Determining the Spin Polarization of Magnetic Tunnel Junctions. *Science* **1999**, *286* (5439), 507–509. https://doi.org/10.1126/science.286.5439.507.

(14) Graziosi, P.; Prezioso, M.; Gambardella, A.; Kitts, C.; Rakshit, R. K.; Riminucci, A.; Bergenti, I.; Borgatti, F.; Pernechele, C.; Solzi, M.; Pullini, D.; Busquets-Mataix, D.; Dediu, V. A. Conditions for the Growth of Smooth La0.7Sr0.3MnO3 Thin Films by Pulsed Electron Ablation. *Thin Solid Films* **2013**, *534*, 83–89. https://doi.org/10.1016/j.tsf.2013.02.008.

(15) Gobbi, M.; Pascual, A.; Golmar, F.; Llopis, R.; Vavassori, P.; Casanova, F.; Hueso, L. E. C60/NiFe Combination as a Promising Platform for Molecular Spintronics. *Organic Electronics* **2012**, *13* (3), 366–372. https://doi.org/10.1016/j.orgel.2011.12.002.

(16) Giannozzi, P.; Baroni, S.; Bonini, N.; Calandra, M.; Car, R.; Cavazzoni, C.; Ceresoli, D.; Chiarotti, G. L.; Cococcioni, M.; Dabo, I.; Corso, A. D.; Gironcoli, S. de; Fabris, S.; Fratesi, G.; Gebauer, R.; Gerstmann, U.; Gougoussis, C.; Kokalj, A.; Lazzeri, M.; Martin-Samos, L.; Marzari, N.; Mauri, F.; Mazzarello, R.; Paolini, S.; Pasquarello, A.; Paulatto, L.; Sbraccia, C.; Scandolo, S.; Sclauzero, G.; Seitsonen, A. P.; Smogunov, A.; Umari, P.; Wentzcovitch, R. M. QUANTUM ESPRESSO: A Modular and Open-Source Software Project for Quantum Simulations of Materials. *J. Phys.: Condens. Matter* **2009**, *21* (39), 395502. https://doi.org/10.1088/0953-8984/21/39/395502.

(17) Li, D.; Barreteau, C.; Kawahara, S. L.; Lagoute, J.; Chacon, C.; Girard, Y.; Rousset, S.; Repain, V.; Smogunov, A. Symmetry-Selected Spin-Split Hybrid States in C60 Ferromagnetic Interfaces. *Phys. Rev. B* **2016**, *93* (8), 085425. https://doi.org/10.1103/PhysRevB.93.085425.

(18) Ma'Mari, F. A.; Moorsom, T.; Teobaldi, G.; Deacon, W.; Prokscha, T.; Luetkens, H.; Lee, S.; Sterbinsky, G. E.; Arena, D. A.; MacLaren, D. A.; Flokstra, M.; Ali, M.; Wheeler, M. C.; Burnell, G.; Hickey, B. J.; Cespedes, O. Beating the Stoner Criterion Using Molecular Interfaces. *Nature* **2015**, *524* (7563), 69–73. https://doi.org/10.1038/nature14621.

(19) Cummings, M.; Gliga, S.; Lukanov, B.; Altman, E. I.; Bode, M.; Barrera, E. V. Surface Interactions of Molecular C60 and Impact on Ni(100) and Co(0001) Film Growth: A Scanning Tunneling Microscopy Study. *Surface Science* **2011**, *605* (1), 72–80. https://doi.org/10.1016/j.susc.2010.10.002.

(20) Zhao, Y.; Liu, X.; Lyu, L.; Li, L.; Tan, W.; Wang, S.; Wang, C.; Niu, D.; Xie, H.; Huang, H.; Gao, Y. Fullerene (C60) Interlayer Modification on the Electronic Structure and the Film Growth of 2,7-Diocty[1]Benzothieno-[3,2-b]Benzothiophene on SiO2. *Synthetic Metals* **2017**, *229*, 1–6. https://doi.org/10.1016/j.synthmet.2017.04.020.

(21) Lee, J. Y. Efficient Hole Injection in Organic Light-Emitting Diodes Using C60 as a Buffer Layer for Al Reflective Anodes. *Appl. Phys. Lett.* **2006**, *88* (7), 073512. https://doi.org/10.1063/1.2174838.

(22) De Teresa, J. M.; Barthélémy, A.; Fert, A.; Contour, J. P.; Lyonnet, R.; Montaigne, F.; Seneor, P.; Vaurès, A. Inverse Tunnel Magnetoresistance in Co/SrTiO3/La0.7Sr0.3MnO3: New Ideas on Spin-Polarized Tunneling. *Phys. Rev. Lett.* **1999**, *82* (21), 4288–4291. https://doi.org/10.1103/PhysRevLett.82.4288.

(23) Velev, J. P.; Belashchenko, K. D.; Stewart, D. A.; van Schilfgaarde, M.; Jaswal, S. S.; Tsymbal, E. Y. Negative Spin Polarization and Large Tunneling Magnetoresistance in Epitaxial Co\SrTiO3\Co Magnetic Tunnel Junctions. *Phys. Rev. Lett.* **2005**, *95* (21), 216601. https://doi.org/10.1103/PhysRevLett.95.216601.

(24) Vera Marún, I. J.; Postma, F. M.; Lodder, J. C.; Jansen, R. Tunneling Magnetoresistance with Positive and Negative Sign in La0.66Sr0.33MnO3/SrTiO3/Co Junctions. *Phys. Rev. B* **2007**, *76* (6), 064426. https://doi.org/10.1103/PhysRevB.76.064426.

(25) Itoh, H.; Inoue, J. Interfacial Electronic States and Magnetoresistance in Tunnel Junctions. *Surface Science* **2001**, *493* (1), 748–756. https://doi.org/10.1016/S0039-6028(01)01294-8.

(26) Tsymbal, E. Y.; Pettifor, D. G. Modelling of Spin-Polarized Electron Tunnelling from 3d Ferromagnets. *J. Phys.: Condens. Matter* **1997**, *9* (30), L411–L417. https://doi.org/10.1088/0953-8984/9/30/002.

(27) Fei, X.; Wu, G.; Lopez, V.; Lu, G.; Gao, H.-J.; Gao, L. Spin-Dependent Conductance in Co/C60/Co/Ni Single-Molecule Junctions in the Contact Regime. *J. Phys. Chem. C* **2015**, *119* (21), 11975–11981. https://doi.org/10.1021/acs.jpcc.5b01763.

(28) Liu, X.; Shi, J. Magnetic Tunnel Junctions with Al2O3 Tunnel Barriers Prepared by Atomic Layer Deposition. *Appl. Phys. Lett.* **2013**, *102* (20), 202401. https://doi.org/10.1063/1.4807132.

(29) Garcia, V.; Bibes, M.; Barthélémy, A.; Bowen, M.; Jacquet, E.; Contour, J.-P.; Fert, A. Temperature Dependence of the Interfacial Spin Polarization of La2/3Sr1/3MnO. *Phys. Rev. B* **2004**, *69* (5), 052403. https://doi.org/10.1103/PhysRevB.69.052403.

(30) Schleicher, F.; Halisdemir, U.; Lacour, D.; Gallart, M.; Boukari, S.; Schmerber, G.; Davesne, V.; Panissod, P.; Halley, D.; Majjad, H.; Henry, Y.; Leconte, B.; Boulard, A.; Spor, D.; Beyer, N.; Kieber, C.; Sternitzky, E.; Cregut, O.; Ziegler, M.; Montaigne, F.; Beaurepaire, E.; Gilliot, P.; Hehn, M.; Bowen, M. Localized States in Advanced Dielectrics from the Vantage of Spin- and Symmetry-Polarized Tunnelling across MgO. *Nat Commun* **2014**, *5* (1), 4547. https://doi.org/10.1038/ncomms5547.

(31) LeClair, P.; Kohlhepp, J. T.; van de Vin, C. H.; Wieldraaijer, H.; Swagten, H. J. M.; de Jonge, W. J. M.; Davis, A. H.; MacLaren, J. M.; Moodera, J. S.; Jansen, R. Band Structure and Density of States Effects in Co-Based Magnetic Tunnel Junctions. *Phys. Rev. Lett.* **2002**, *88* (10), 107201. https://doi.org/10.1103/PhysRevLett.88.107201.

(32) Pruneda, J. M.; Ferrari, V.; Rurali, R.; Littlewood, P. B.; Spaldin, N. A.; Artacho, E. Ferrodistortive Instability at the (001) Surface of Half-Metallic Manganites. *Phys. Rev. Lett.* **2007**, *99* (22), 226101. https://doi.org/10.1103/PhysRevLett.99.226101.

(33) Thomas, A.; Moodera, J. S.; Satpati, B. Evidence for Positive Spin Polarization in Co with SrTiO3 Barriers. *Journal of Applied Physics* **2005**, *97* (10), 10C908. https://doi.org/10.1063/1.1850400.

For Table of Contents Use Only

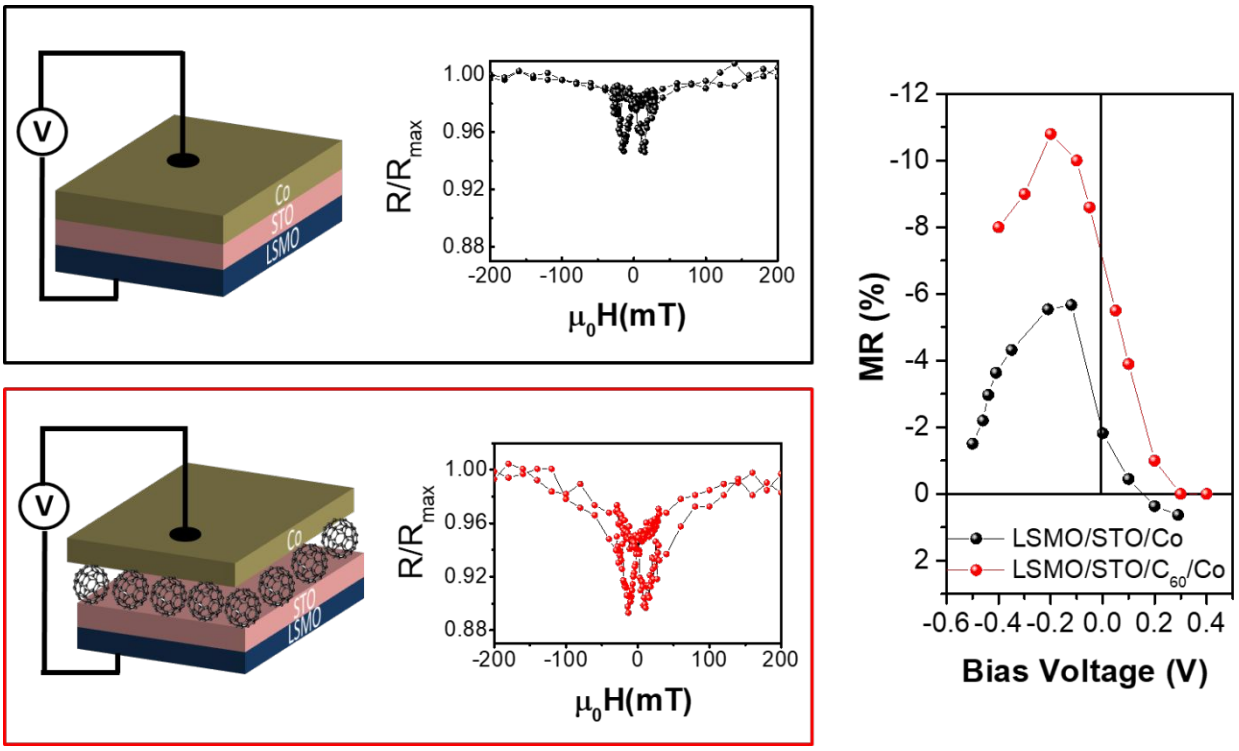

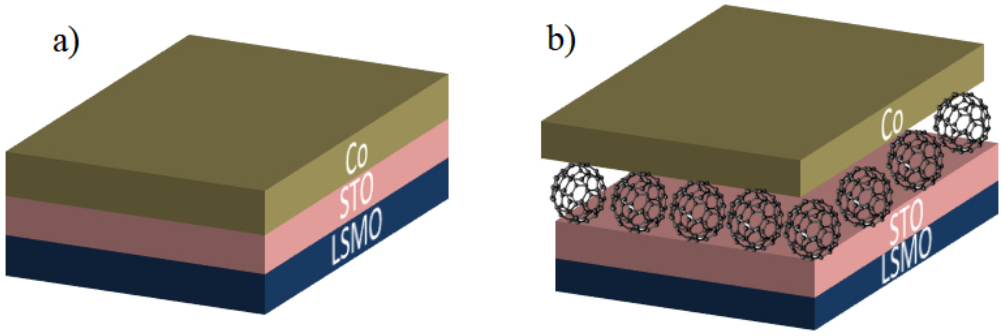

Schematic drawing of MTJ junctions. a) Reference device $La_{0.7}Sr_{0.3}MnO_3$ /$SrTiO_3$ /C_{60}/ b) C_{60}/ seeded MTJ

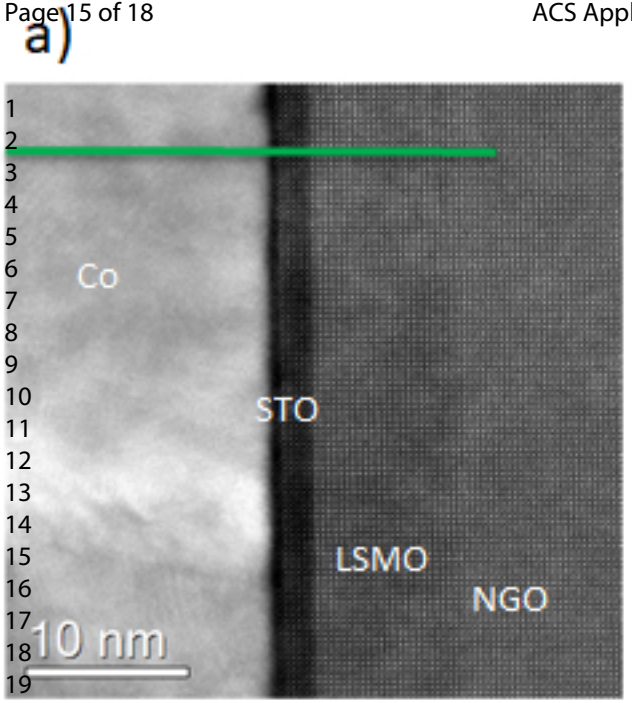
a)
Co
STO
LSMO
NGO
10 nm

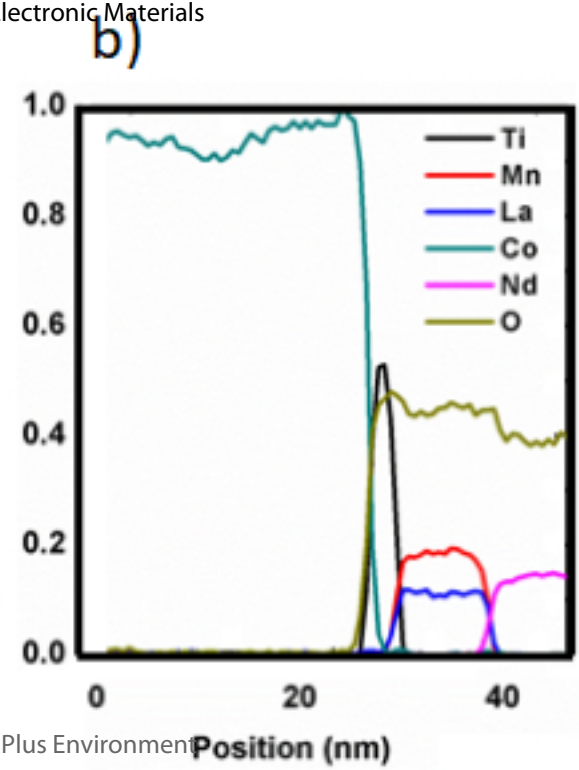
b)
1.0
0.8
0.6
0.4
0.2
0.0
0
20
40
Position (nm)
Ti
Mn
La
Co
Nd
O

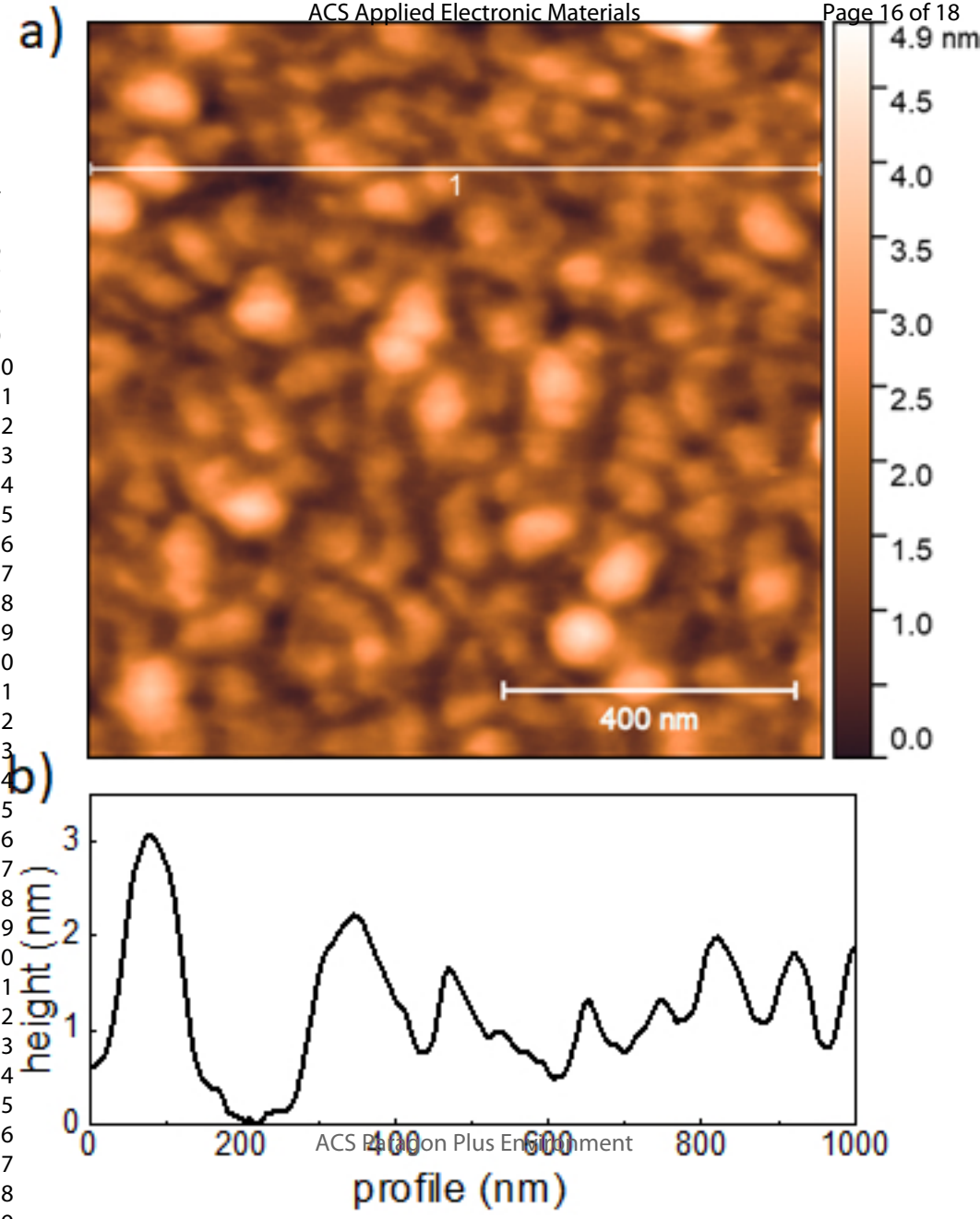

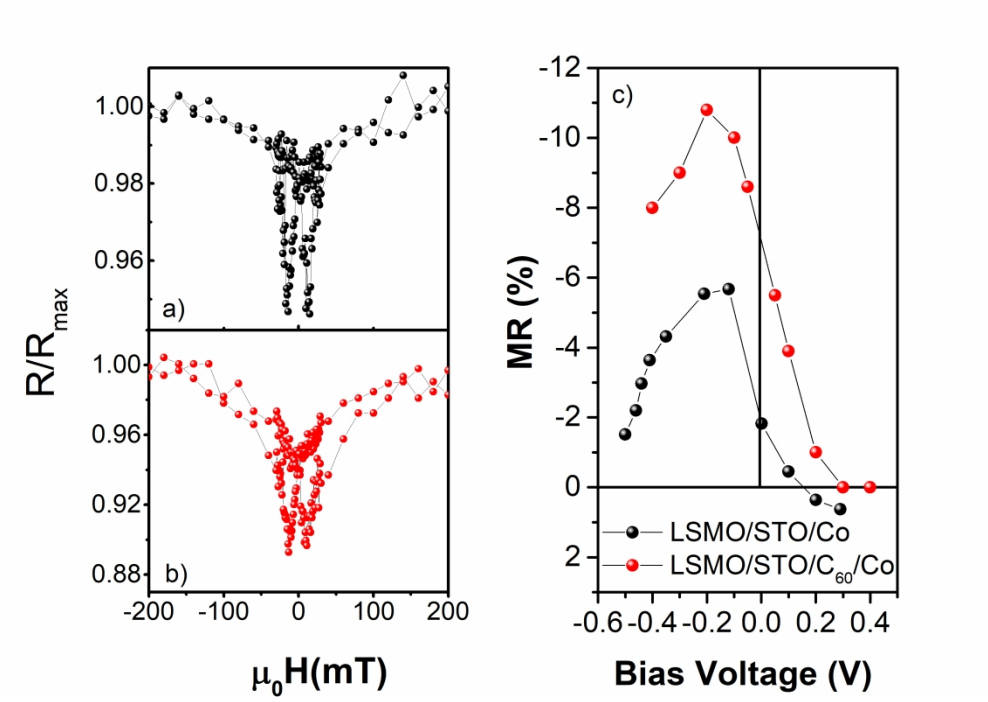

Negative Tunneling magnetoresistance (TMR) as a function of applied field for the two junctions LSMO/STO/Co(a) and LSMO/STO/C_{60}/Co(b) measured with voltage bias of 100 mV (c) TMR ratio as a function of the applied dc bias for LSMO/STO/Co junctions (black balls) and LSMO/STO/C_{60}/Co (red balls). Errors bars are within the symbol size.

289x202mm (300 x 300 DPI)

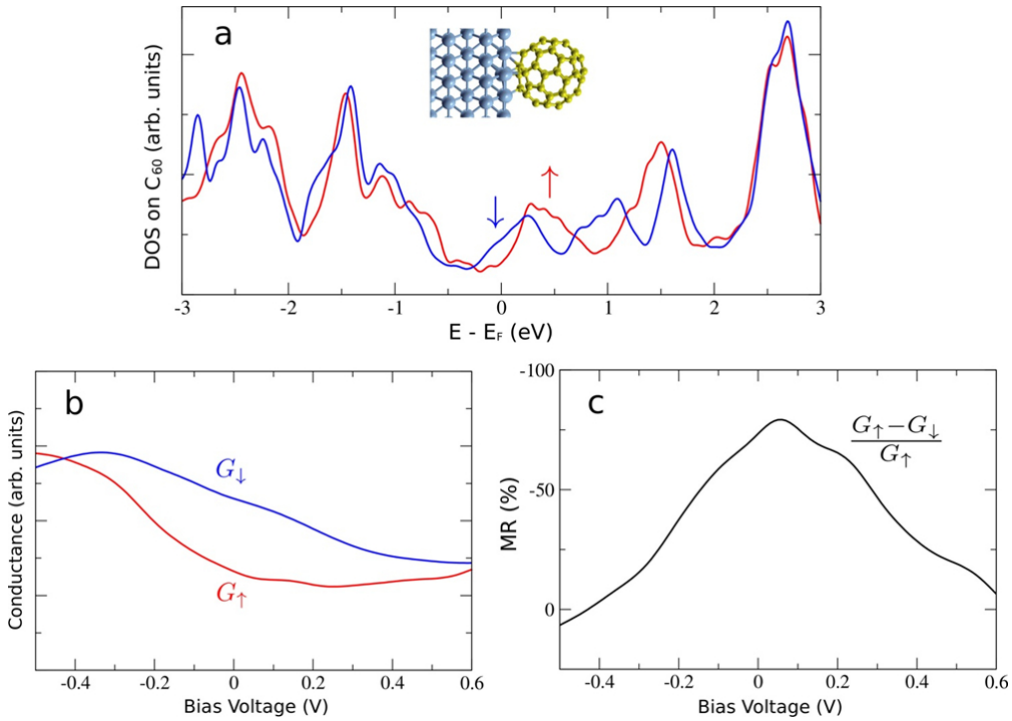

hcp-Co/C60 interface with C60in (5:6)-bond adsorption geometry: a) Spin-resolved PDOS on the C60 molecule; b) Spin-resolved conductance calculated from the integrated PDOS; c) Calculated interface TMR (G↑-G↓)/G↑. Spin-up and -down components in a) and b) are plotted in blue and red, respectively. In b) and c) negative/positive voltage corresponds to probing occupied/unoccupied states.

170x120mm (149 x 149 DPI)

Supporting Information

Spinterface effects in hybrid $La_{0.7}Sr_{0.3}MnO_3$ /$SrTiO_3$ /C_{60}/Co magnetic tunnel junctions

Ilaria Bergenti[1], Takeshi Kamiya[2], Dongzhe Li[3] Alberto Riminucci[1], Patrizio Graziosi[1], Donald .A. MacLaren[4], Rajib K. Rakshit [5], Manju Singh [5], Mattia Benini[1], Hirokazu Tada[2], Alexander Smogunov[6], Valentin A. Dediu[1]*

ilaria.bergenti@cnr.it

[1] Institute of Nanostructured Materials ISMN-CNR, Via Gobetti 101, Bologna 40129, Italy

[2] Department of Materials Engineering Science, Osaka University, 1-3, Machikaneyama, Toyonaka, Osaka, Japan, 560-8531

[3] CEMES, Université de Toulouse, CNRS, 29 rue Jeanne Marvig, F-31055 Toulouse, France

[4] SUPA, School of Physics and Astronomy, University of Glasgow, Glasgow G12 8QQ

[5] CSIR - National Physical Laboratory, Dr. K. S. Krishnan Marg, New Delhi, 110012, India

[6]Service de Physique de l'Etat Condensé (SPEC), CEA, CNRS, Université Paris-Saclay, CEA Saclay 91191 Gif-sur-Yvette Cedex, France

S1: C60 molecules adsorbed on STO: AFM characterization

Upon deposition of approximately 2 ML C_{60} (2nm) onto a STO substrate at RT, islands are formed having a typical size of several tens of nanometers in diameter. Figure S1 shows a representative AFM image of the STO substrate (RMS=0.1±0.05 nm)) and of the 2nm C60 on STO. As can be seen from the height profile shown in Fig. S2 , the prevalent height of the islands is 1.5 nm corresponding to nearly double-layer C60 islands. Statistical analysis of surface coverage of the thin films indicated that 95% of the analyzed surface is covered by C_{60}.

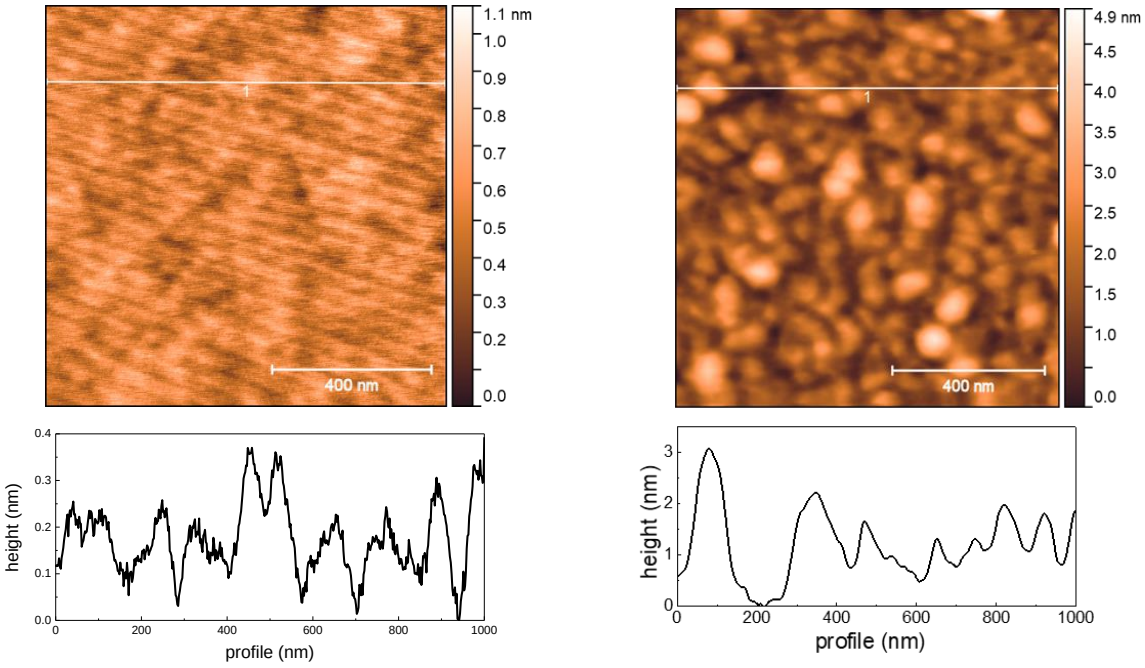

Figure S1: Surface morphology obtained by AFM: STO substrate (right) and 2 nm C_{60} on STO (left). Bottom lines represent line profiles as indicated by the white lines

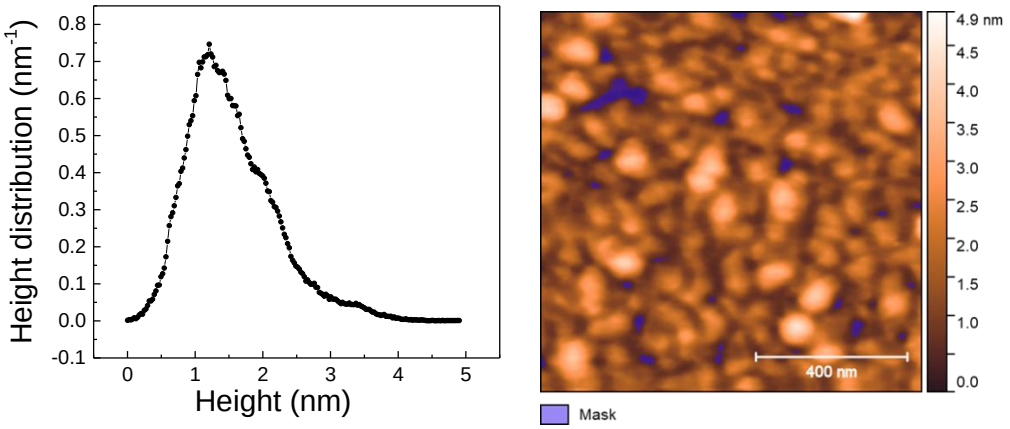

Figure S2: (left) Height analysis for C_{60} islands in the AFM images for 2nm thick c60 layer. (right) Total C60 coverage calculated by masking height below 0.5 nm on the height scales (coverage 98%).

S2: Temperature dependent I-V curves

Temperature-dependent I–V characteristics of LSMO/STO/Co MTJ with a nominal STO thickness of 5nm are shown in fig. S3 All the plots depict nonlinear and quasi-symmetric I–V characteristics. The R(T) curve exhibits a smooth increase of the resistance on lowering temperature compatible with direct tunneling transport. However, R(T) exhibits a peak with a maximum at about 200 K(fig S3, blackballs) that seems to be a common feature in LSMO/STO/Co MTJs and whose origin is not well established yet.[1]. In case of C_{60} insertion, the R(T) exhibits a purely insulating behavior, without traces of the LSMO contribution. The change in R(T) in case of C60 insertion is also an indication of the effectiveness of the molecular layer in transport, excluding the metal penetration through the molecular layer and the subsequent molecular damage that typically result in behavior characteristic of electronic shorts

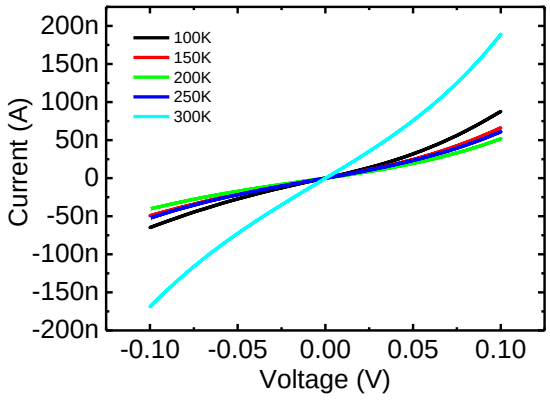

Figure S3: I-V measurements for the reference sample LSMO(15nm)/STO(5nm)/Co(50nm), without applying an external magnetic field.

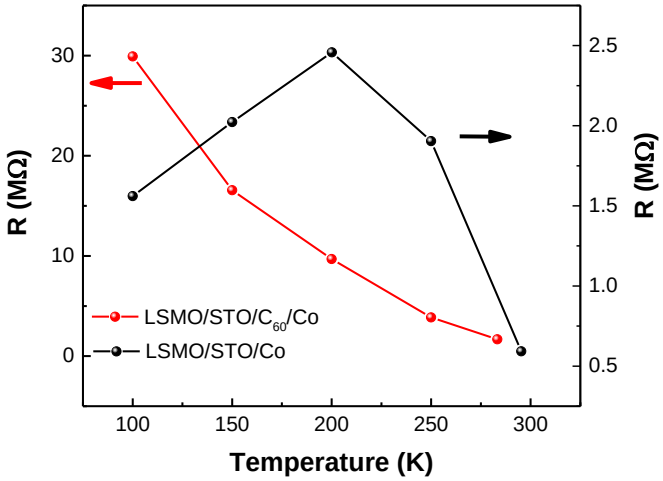

Figure S4: Temperature dependence of the MTJ resistance

S3: Temperature dependent MR

The temperature dependence of the TMR in the LSMO based junctions decays rapidly and vanishes below the Curie temperature of LSMO layer that is close to 320K for such 15 nm thick layer[2]. Since tunneling reflects mainly the properties of the electrode/barrier interface, this behavior has been ascribed to a premature loss of the spin polarization at interfaces. This is consistent with the weakening of the ferromagnetism of LSMO[3].

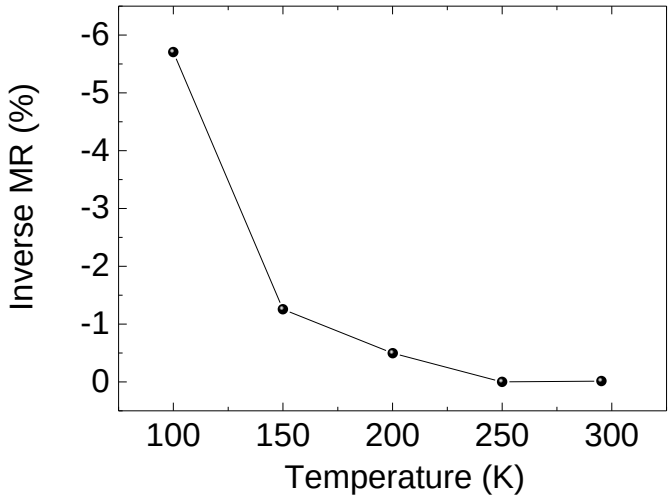

Figure S5: Temperature dependence of the MR resistance for LSMO/STO/Co MTJ measured at bias V=-0.1 V

(1) Sun, J. Z.; Roche, K. P.; Parkin, S. S. P. Interface Stability in Hybrid Metal-Oxide Magnetic Trilayer Junctions. *Phys. Rev. B* **2000**, *61* (17), 11244–11247. https://doi.org/10.1103/PhysRevB.61.11244.

(2) Garcia, V.; Bibes, M.; Barthélémy, A.; Bowen, M.; Jacquet, E.; Contour, J.-P.; Fert, A. Temperature Dependence of the Interfacial Spin Polarization of La2/3Sr1/3MnO. *Phys. Rev. B* **2004**, *69* (5), 052403. https://doi.org/10.1103/PhysRevB.69.052403.

(3) Park, J.-H.; Vescovo, E.; Kim, H.-J.; Kwon, C.; Ramesh, R.; Venkatesan, T. Magnetic Properties at Surface Boundary of a Half-Metallic Ferromagnet La0.7Sr0.3MnO3. *Phys. Rev. Lett.* **1998**, *81* (9), 1953–1956. https://doi.org/10.1103/PhysRevLett.81.1953.

Supporting Information

Spinterface effects in hybrid $La_{0.7}Sr_{0.3}MnO_3$ /$SrTiO_3$ /C_{60}/Co magnetic tunnel junctions

Ilaria Bergenti[1], Takeshi Kamiya[2], Dongzhe Li[3] Alberto Riminucci[1], Patrizio Graziosi[1], Donald .A. MacLaren[4], Rajib K. Rakshit [5], Manju Singh [5], Mattia Benini[1], Hirokazu Tada[2], Alexander Smogunov[6], Valentin A. Dediu[1]*

ilaria.bergenti@cnr.it

[1] Institute of Nanostructured Materials ISMN-CNR, Via Gobetti 101, Bologna 40129, Italy

[2] Department of Materials Engineering Science, Osaka University, 1-3, Machikaneyama, Toyonaka, Osaka, Japan, 560-8531

[3] CEMES, Université de Toulouse, CNRS, 29 rue Jeanne Marvig, F-31055 Toulouse, France

[4] SUPA, School of Physics and Astronomy, University of Glasgow, Glasgow G12 8QQ

[5] CSIR - National Physical Laboratory, Dr. K. S. Krishnan Marg, New Delhi, 110012, India

[6]Service de Physique de l'Etat Condensé (SPEC), CEA, CNRS, Université Paris-Saclay, CEA Saclay 91191 Gif-sur-Yvette Cedex, France

S1: C60 molecules adsorbed on STO: AFM characterization

Upon deposition of approximately 2 ML C_{60} (2nm) onto a STO substrate at RT, islands are formed having a typical size of several tens of nanometers in diameter. Figure S1 shows a representative AFM image of the STO substrate (RMS=0.1±0.05 nm)) and of the 2nm C60 on STO. As can be seen from the height profile shown in Fig. S2 , the prevalent height of the islands is 1.5 nm corresponding to nearly double-layer C60 islands. Statistical analysis of surface coverage of the thin films indicated that 95% of the analyzed surface is covered by C_{60}.

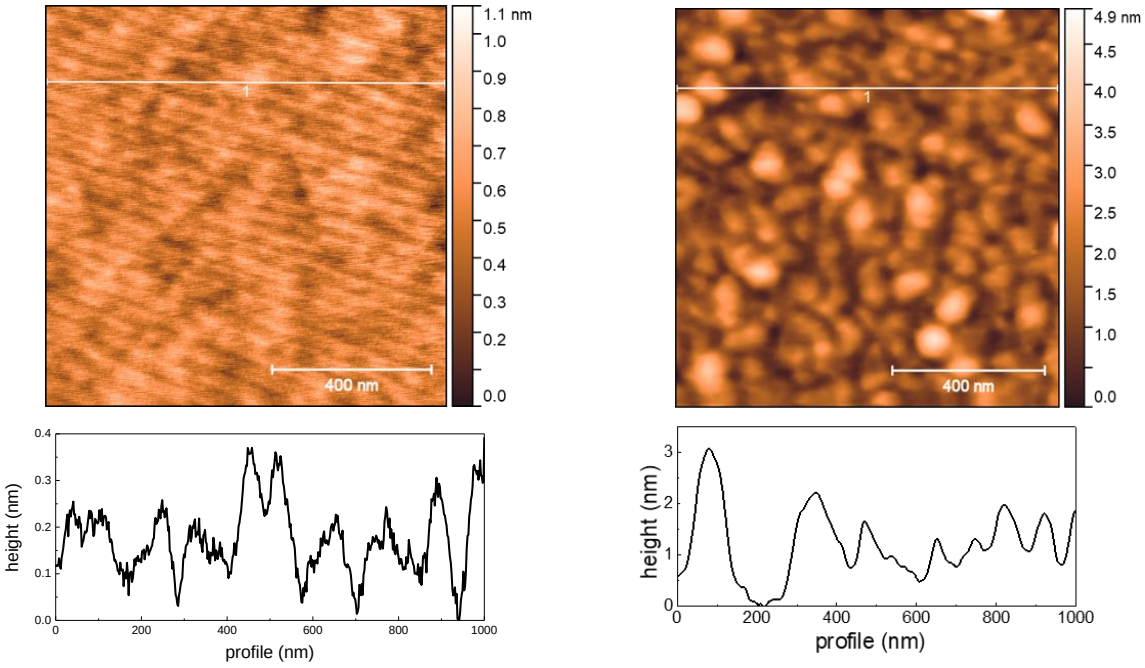

Figure S1: Surface morphology obtained by AFM: STO substrate (right) and 2 nm C_{60} on STO (left). Bottom lines represent line profiles as indicated by the white lines

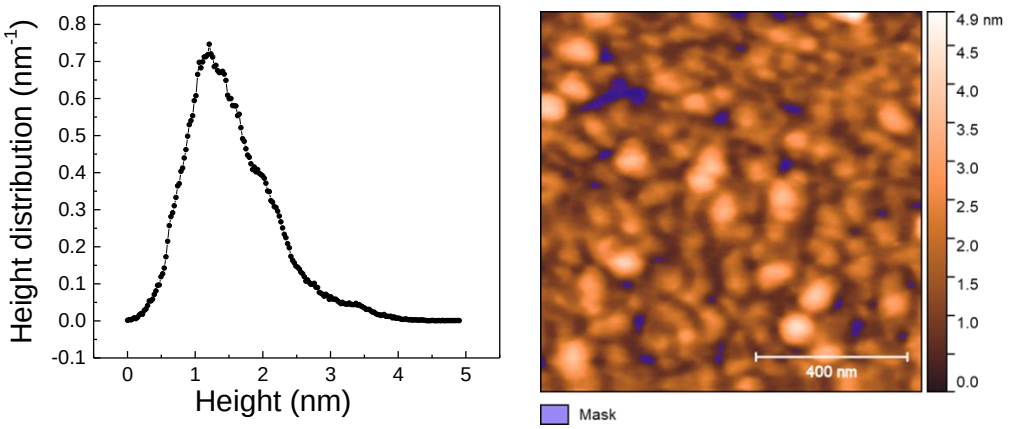

Figure S2: (left) Height analysis for C_{60} islands in the AFM images for 2nm thick c60 layer. (right) Total C60 coverage calculated by masking height below 0.5 nm on the height scales (coverage 98%).

S2: Temperature dependent I-V curves

Temperature-dependent I–V characteristics of LSMO/STO/Co MTJ with a nominal STO thickness of 5nm are shown in fig. S3 All the plots depict nonlinear and quasi-symmetric I–V characteristics. The R(T) curve exhibits a smooth increase of the resistance on lowering temperature compatible with direct tunneling transport. However, R(T) exhibits a peak with a maximum at about 200 K(fig S3, blackballs) that seems to be a common feature in LSMO/STO/Co MTJs and whose origin is not well established yet.[1]. In case of C_{60} insertion, the R(T) exhibits a purely insulating behavior, without traces of the LSMO contribution. The change in R(T) in case of C60 insertion is also an indication of the effectiveness of the molecular layer in transport, excluding the metal penetration through the molecular layer and the subsequent molecular damage that typically result in behavior characteristic of electronic shorts

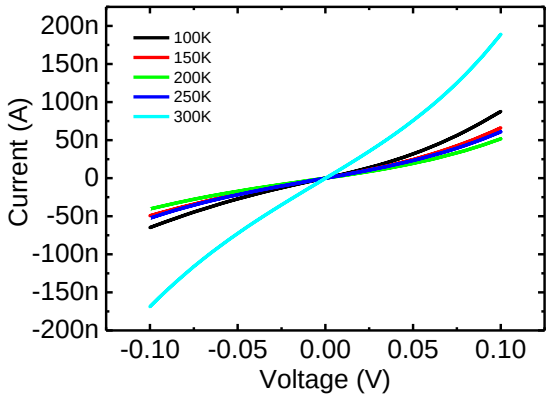

Figure S3: I-V measurements for the reference sample LSMO(15nm)/STO(5nm)/Co(50nm), without applying an external magnetic field.

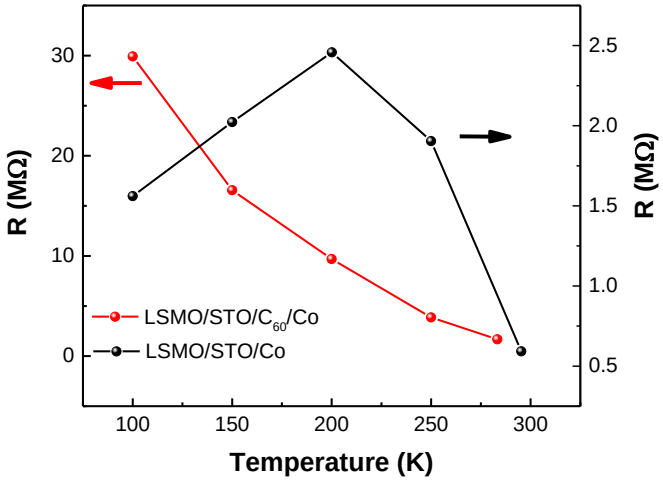

Figure S4: Temperature dependence of the MTJ resistance

S3: Temperature dependent MR

The temperature dependence of the TMR in the LSMO based junctions decays rapidly and vanishes below the Curie temperature of LSMO layer that is close to 320K for such 15 nm thick layer[2]. Since tunneling reflects mainly the properties of the electrode/barrier interface, this behavior has been ascribed to a premature loss of the spin polarization at interfaces. This is consistent with the weakening of the ferromagnetism of LSMO[3].

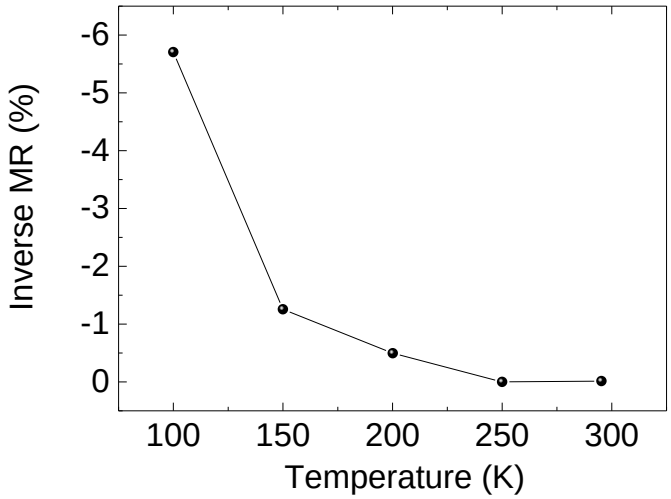

Figure S5: Temperature dependence of the MR resistance for LSMO/STO/Co MTJ measured at bias V=-0.1 V

(1) Sun, J. Z.; Roche, K. P.; Parkin, S. S. P. Interface Stability in Hybrid Metal-Oxide Magnetic Trilayer Junctions. *Phys. Rev. B* **2000**, *61* (17), 11244–11247. https://doi.org/10.1103/PhysRevB.61.11244.

(2) Garcia, V.; Bibes, M.; Barthélémy, A.; Bowen, M.; Jacquet, E.; Contour, J.-P.; Fert, A. Temperature Dependence of the Interfacial Spin Polarization of La2/3Sr1/3MnO. *Phys. Rev. B* **2004**, *69* (5), 052403. https://doi.org/10.1103/PhysRevB.69.052403.

(3) Park, J.-H.; Vescovo, E.; Kim, H.-J.; Kwon, C.; Ramesh, R.; Venkatesan, T. Magnetic Properties at Surface Boundary of a Half-Metallic Ferromagnet La0.7Sr0.3MnO3. *Phys. Rev. Lett.* **1998**, *81* (9), 1953–1956. https://doi.org/10.1103/PhysRevLett.81.1953.